Teleseismic Source Process of The October 30, 2020 Kuşadasi Gulf –İzmir (Turkey) Earthquake (M_w=6.8)

Murat Utkucu[1,2] (iD), Emrah Budakoğlu[1*] (iD), Şefik Ramazanoğlu[1] (iD)

[1]*Sakarya University Engineering Faculty Department of Geophysics 54187, Serdivan, SAKARYA*
[2]*Sakarya University, Disaster Management Application and Research Center, Serdivan, SAKARYA*

Abstract

The October 30, 2020 Kuşadası Gulf-İzmir earthquake took place along a fault bounding Kuşadası Gulf in the South causing significant damage and loss of life, especially in İzmir city. The earthquake damage due to the strong ground motion is augmented by a tsunami that caused a water inundation. In the present study the source properties of the earthquake are investigated by inverting teleseismic *P* waveforms. The complex waveforms are fit with two subevents in the point-source inversion that requires dominant normal faulting along a roughly E-W trending normal fault dipping north. The finite-source inversion shows that the earthquake is due to failure of a two asperities with slip as high as 2.4 m and the rupture covers a fault area of 30 km x 20 km with unilateral propagation toward west. The finite-source model defines two asperities that are located at hypocentral area and shallow depths near the west top corner of the fault. The earthquake rupture lasts for 17 s and released a seismic moment of 2.21 x 10^{19} Nt.m (M_W=6.83). Presence of a shallow asperity indicates that rupture reaches to the sea bottom which provides a reasonable explanation for the damaging tsunami.

Key words: The 2020 Kuşadası Gulf-İzmir earthquake, teleseismic point-source inversion, teleseismic finite-source inversion, Extensional tectonics.

1. Introduction

The general tectonic setting of Western Turkey and Aegean Sea region is mainly affected by The North Anatolian Fault Zone (NAFZ) in the North and subduction of the African plate beneath the Anatolian plate along the Crete and Cyprus trenches in the South (Figure 1). The subduction related tectonic pull results in westward movement of Anatolian Plate along the NAFZ with increasing velocity and counter clockwise rotation [1, 2]. This general tectonic framework causes an extensional tectonic regime in western Anatolia and under the Aegean Sea with multidirectional extensional structures [3-8]. Kuşadası Gulf is one of these extensional structures extending roughly in E-W direction and is characterised by N-S extension (Figure 2).

The October 30, 2020, Kuşadası Gulf-İzmir earthquake took place along a normal fault bounding Kuşadası Gulf of in the South [9-10]. The source mechanism of the earthquake determined from the seismological data indicated normal faulting along a nearly E-W striking fault (Table 1). The earthquake caused 115 fatalities, hundreds of injured peoples and collapse

---

and damage of the buildings in İzmir, one of the largest city in Turkey. The earthquake also produced a tsunami that caused a water inundation that augmented the damage [11]. The earthquake source region and surrounding has been seismicaly active area both in historical and instrumental period with damaging earthquakes (Figure 2) [12, 13]. This can historically be examplified by the 1668 İzmir, 1881 Çeşme and 1899 Büyük Menderes-Aydın earthquakes. Many large earthquake also struck the area in the instrumental period, including the 1949 and 2017 Karaburun and 1955 Söke earthquakes (Figure 2) [14, 15]. Further several M 5.4-5.9 earthquakes after 1990 also shook the area with light damage [16].
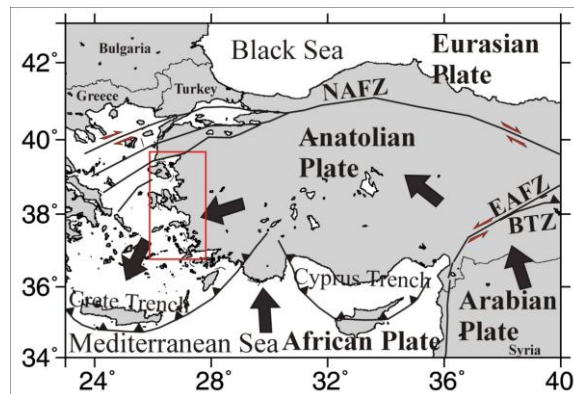
Figure 1. General tectonic setting of Turkey. The red rectangle encloses the fault area shown in *Figure 2*
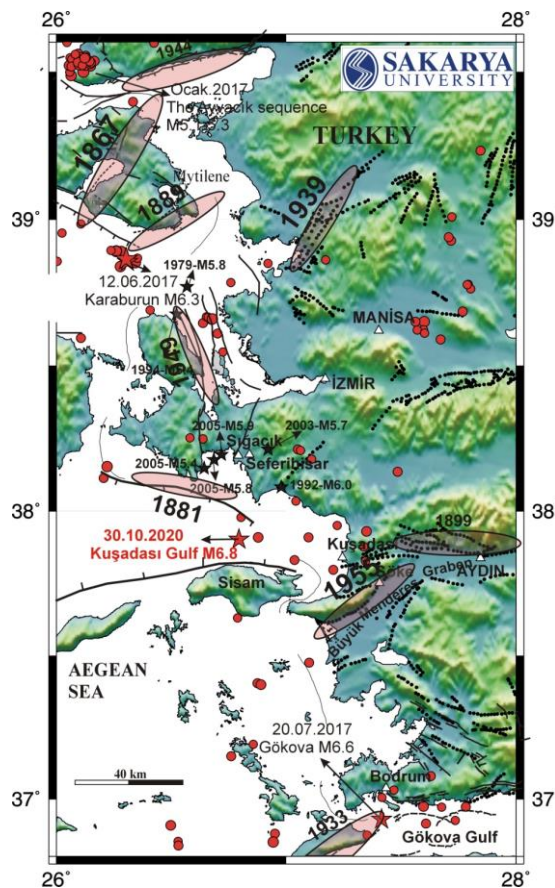
Figure 2. Seismotectonic map of the 2020 Kuşadası Gulf-İzmir earthquake source region. The star shows significant earthquakes' epicentres while the pink shaded ellipses denote rupture extends of the labelled earthquakes. Red circles represent epicentres of M≥4.0 earthquakes from Kandilli Observatory and Earthquake Research Institute Catalogue between January 2010 and April 2017

Table 1. Source parameters of the October 30, 2020 Kuşadası Gulf-İzmir earthquake

|	KOERI[1]	AFAD[2]	USGS NEIC	GCMT	This study (point-source inversion)		
					Subevent1	Subevent2	Total
Origin	11:51:24	11:51:24	11:51:27				
Latitude (º)	37.9020	37.8881	37.918				
Longitude (º)	26.7942	26.7770	26.790				
Depth (km)	12	16.5	21				
Strike (º)			276	270	256	258	251
Dip (º)			29	37	49	34	41
Rake(º)			-88	-95	-66	-116	-102
M_o ($\times 10^{19}$Nm)			4.09	4.01	0.70	1.07	1.55
M_W	6.9		7.01	7.01	6.50	6.62	6.75
CMT depth (km)			11.5	12	12	20	
Centroid time				**11:51:34.8**			

[1] Kandilli Observatory and Earthquake Research Institute
[2] Disaster and Emergency Management Presidency

In the present study the source process of the earthquake will be illuminated using the teleseismic point- and finite-source inversions. Since the earthquake caused significant structural damage, determination of the source properties would be valuable in studying the strong-ground motion and modelling of the tsunami.

2. Teleseismic data

The teleseismic broadband P waveforms from stations having epicentral distances between 30º and 90º are used for the teleseismic source inversions. The data have been downloaded from IRIS Data Management Centre. The waveforms are bandpass filtered from 0.01 to 0.5 Hz and resampled at 0.5 s time interval. The data comprise 14 P displacement waveforms, onsets of which are determined from the time tables of Jeffreys and Bullen [17]. The record lengths selected for both point- and finite-source inversions are 50 s. The data has a good coverage around the source (Figure 3).
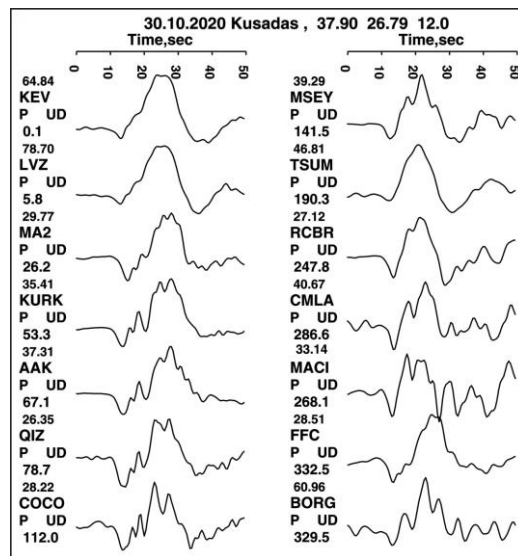
Figure 3. The teleseismic P displacement waveforms at 14 stations that used in the inversions. Note that waveforms are drawn 10 s before the first arrivals and bandpass filtered between 0.01 and 1.0 Hz

## 3. Teleseismic source inversion methods

3.1. Point-source inversion

The point-source inversion methodology of Kikuchi and Kanamori [18] is utilized. The earthquake rupture has been approximated by a vertical grid of 12x5 point-sources along the strike and dip, respectively (Figure 4). The point source spacing is 4 km for both strike and dip directions. The orientation of grid (strike) scheme is taken as 276º (Table 1). The point sources are represented by a moment tensor, components of which are iteratively determined. The crustal structure given by Özer and Polat [19]. (Table 2) and a trapezoid source-rise time function with 2 s rise and fall and 8 s total duration are used in the calculations of the synthetics. The rupture velocity is taken as 3.3 km/sec. Regarding complexity of the waveforms (Figure 3) modelling is carried out using multiple subevents and the observed waveforms are fit sufficiently using two subevents. The results are shown in Figures 4 and 5 and subevent source parameters are listed in Table 1.

Table 2. Crustal velocity structure used in the waveform inversions (Özer and Polat [19])

Thickness(km)	V_P (km/sec)	V_S (km/sec)	ρ (kg/m^3)
7.0	4.75	2.75	2660
8.0	6.20	3.29	2750
9.0	6.80	3.89	2900
-	7.70	4.45	3300
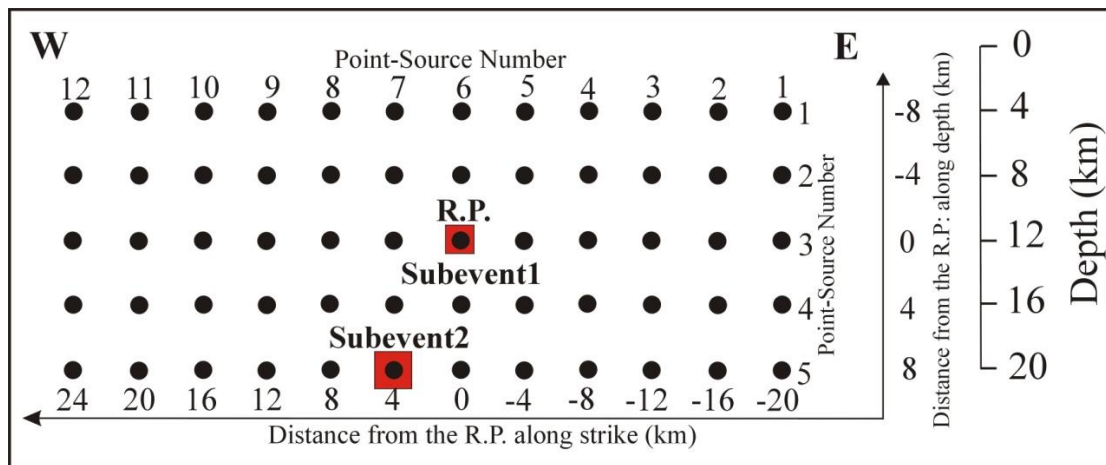
Figure 4. Point-source grid scheme used in the point-source inversion along with the subevent locations resulted from the inversion. See Table 1 for the subevent source parameters. **R.P.**: Rupture Point
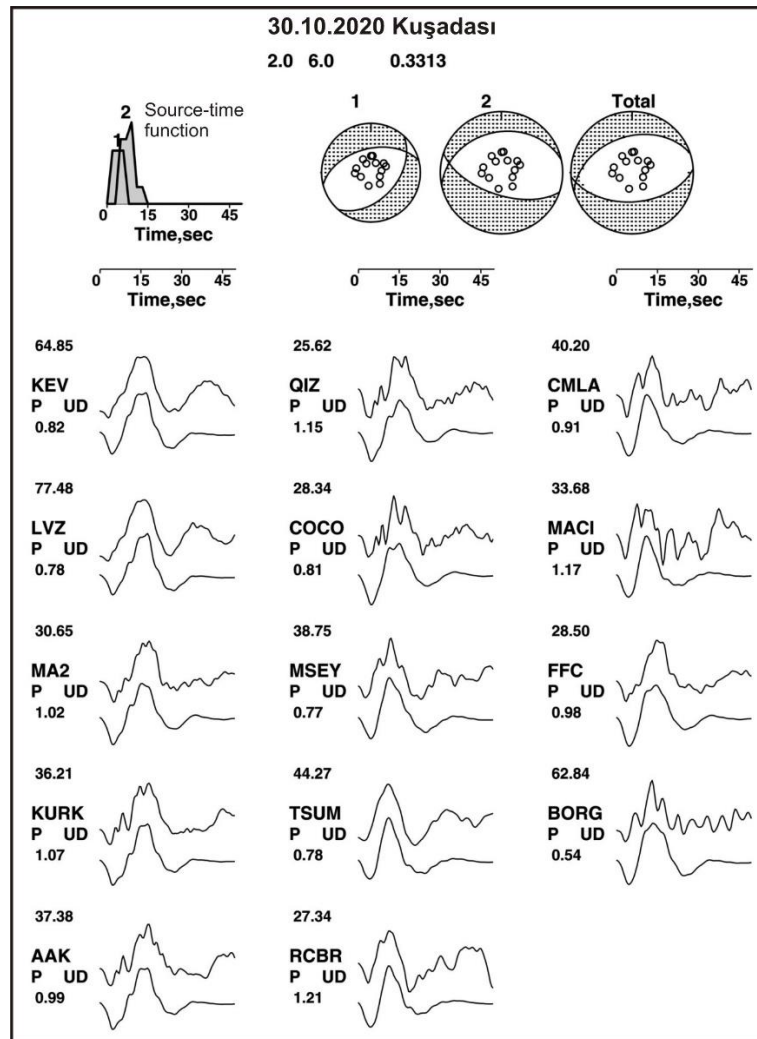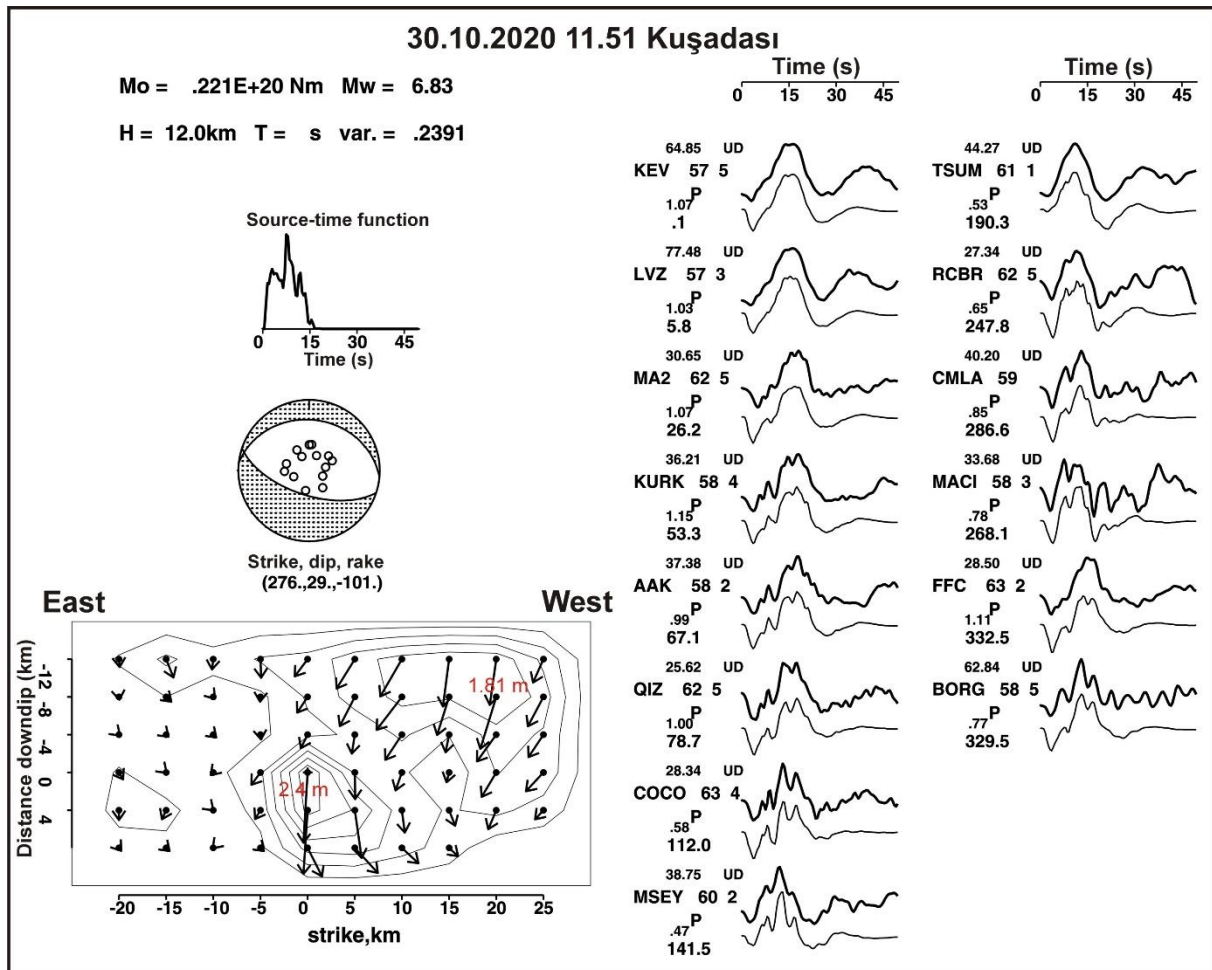
Figure 5. The point-source inversion results showing source time function, subevent source mechanisms and synthetic-observed waveform comparison

3.2. Finite-source inversion

For the finite-source modelling inversion technique developed by Kikuchi et al. [20] is used. The target earthquake is represented by equally spaced (4 km) 10 x 6 grid points along the strike and the dip, respectively. The strike, dip and rake angles of the grid plane are based on the available source mechanisms (Table 1). The Green's functions for the grid points are calculated using the method given by Koketsu [21] and the velocity structure defined in Table 2. The strike, dip and rake angle of the grid plane are taken as 276º, 29º and -88º, respectively (Table 1). The rake angle can vary ±45º of the defined value in the modelling. The modelling is carried out by incorporating 5 time windows with isosceles triangle rise-time functions of 1.0 s rise and fall. A maximum rupture velocity of 3.3 km/s is defined for the modelling. Though the source parameters resulted from point-source inversion in the present study (Table 1) is also tried in the inversion it is seen that using a grid plane with the source parameters given by the USGS NEIC provides better fit to the data. The results of the finite-source inversion are shown in Figure 6.

Figure 6. The finite-source inversion results showing source time function, source mechanism, slip distribution and synthetic-observed waveform comparison

4. Discussion

The point-source inversion results suggest that the earthquake rupture consists of two subevents both having dominant normal fault mechanisms (Table 2; Figures 4 and 5). The earthquake rupture started with a subevent at hypocentre at 12 km depth. The seismic moment release of the first subevent lasts 8 s with a seismic moment of 7×10^{18} Nt.m (M_W=6.5). The second subevent is larger than the first one and is located at 20 km depth and 4 km west of the of the first subevent. Its rupture starts 3 s after the earthquake rupture initiation, lasts 12 s and releases a seismic moment of 1.07×10^{19} Nt.m (M_W=6.62). Regarding aftershock distribution (KOERI 2020) northerly dipping rupture planes in the source mechanisms are selected as the fault planes in coincidence with the fault bounding the Kuşadası Gulf in the south. The whole earthquake rupture takes place in 15 s and corresponds to a total seismic moment release of 1.55×10^{19} Nt.m (M_W=6.75).

Figure 6, in which the finite-source inversion results are shown, suggests that the earthquake is due to failure of a two asperities and the rupture covers a fault area of 30 km x 20 km. The rupture is unilateral to the west (or toward the sea) and propagated updip from the hypocentre to the top western corner of the fault. The asperity at the hypocentral area is nearly circular in shape with 10 km in diameter and slips as high as 2.4 m. The other asperity is located over a shallow fault area and covers a rectangular fault area of 20 km by 8 km with a peak slip of 1.8 m. The rupture lasts for 17 s and slip vectors obtained indicate dominantly vertical slip with the

fault block beneath the Kuşadası Gulf or hanging wall is down. A seismic moment of 2.21 x 10^{19} Nt.m (M_W=6.83) is calculated for the slip model. Presence of a shallow asperity indicates that rupture reaches to the sea bottom which provides a reasonable explanation for the damaging tsunami.

2020 Kuşadası Gulf-İzmir earthquake shows similarities with the July 20, 2017 Bodrum-Kos earthquake (M_W=6.6). The 2017 Bodrum-Kos earthquake also occurred along a E-W trending normal fault that bounds Gökova Basin in the south and caused a damaging tsunami [22, 23]. Nonetheless, the 2020 Kuşadası Gulf-İzmir earthquake is notably larger and its rupture seems to be more complex than the 2017 Bodrum-Kos earthquake. Both earthquakes have shown importance of tsunami hazard along the Turkish coasts.

5. Conclusions

The teleseismic body waveforms of the October 30, 2020 Kuşadası Gulf-İzmir earthquake are inverted using both point- and finite-source inversion techniques to study the source process. The point-source inversion results indicate two subevents with dominant normal faulting along a roughly E-W trending normal fault dipping north. Failure of a two asperities with slip as high as 2.4 m is apparent from the slip model resulted from the finite-source inversion. One asperity is located at hypocentral area while the other one is located at shallow depths near the west top corner of the fault. The rupture covers a fault area of 30 km x 20 km with unilateral propagation toward west and lasts for 17 s, releasing a seismic moment of 2.21 x 10^{19} Nt.m (M_W=6.83).

References

[1]   Reilinger, R., McClusky, S., Vernant, P., Lawrence, S., Ergintav, S., Cakmak, R., et al. GPS constraints on continental deformation in the Africa-Arabia-Eurasia continental collision zone and implications for the dynamics of plate interactions. Journal of Geophysical Research: Solid Earth, 2006; 111-B5.

[2]   Jolivet, L., Faccenna, C., Huet, B., Labrousse, L., Le Pourhiet, L., Lacombe, O., et al. Aegean tectonics: Strain localisation, slab tearing and trench retreat. Tectonophysics, 2013; 597, 1-33.

[3]   Koçyiğit, A. Tectonis of Hoyran Lake (Isparta Bend) region, Türk Jeol. Kurumu Bül., 1983; 26, 1-10 (in Turkish).

[4]   Koçyiğit, A. Güneybatı Türkiye ve yakın dolayının levha içi yeni tektonik gelişim, Türkiye Jeol. Kur. Bült., 1984; 27, 1-16 (in Turkish).

[5]   Jackson, J. and McKenzie, D. P. Active tectonics of the Alpine-Himalayan belt between western Turkey & Pakistan, Geophysical Journal International, 1984; 77(1), 185-264.

[6]   Eyidoğan, H. and Jackson, J. A seismological study of normal faulting in the Demirci, Alaşehir and Gediz earthquakes of 1969–70 in western Turkey: Implications for the nature and geometry of deformation in the continental crust. Geophysical Journal International, 1985; 81(3), 569-607.

[7]   Taymaz, T., Jackson, J. and McKenzie, D. Active tectonics of the north and central Aegean Sea. Geophysical Journal International, 1991; 106(2), 433-490.

[8]   Aktuğ, B., Nocquet, J. M., Cingöz, A., Parsons, B., Erkan, Y., England, P. et al. A. Deformation of western Turkey from a combination of permanent and campaign GPS data: Limits to block-like behavior. Journal of Geophysical Research: Solid Earth, 2009; 114(B10).

[9]   KOERI (Kandilli Observatory and Earthquake Research Institute), 30 Ekim 2020 Ege Denizi Depremi Basın Bülteni, 2020; 8 sf.

[10] AFAD (Disaster and Emergency Management Presidency), 30 Ekim 2020 Ege Denizi, Seferihisar (İzmir) Açıkları (17,26 Km) Mw=6.6 Depremine İlişkin Ön Değerlendirme Raporu, 2020; 10 sf.

[11] Yalçıner, A. C., Doğan, G. G., Ulutaş, E., Polat, O., Tarih, A., Yapar, E. R. et al. The 30 October 2020 (11:51 Utc) İzmır-Samos Earthquake and Tsunami; Post-Tsunami Field Survey Preliminary Results, 2020; 33 pp.

[12] Papazachos B.C. and Papazachou C.B. The earthquakes of Greece. Ziti Publication, Thessaloniki, 1997; 304 pp.

[13] Ambraseys, N. Earthquakes in the Mediterranean and Middle East: a multidisciplinary study of seismicity up to 1900. Cambridge University Press, 2009.

[14] Kalafat, D., Kekovalı, K., Güneş, Y., Yılmazer, M., Kara, M., Deniz, P., et al. A Cataloque of Source Parameters of Moderate and Strong Earthquakes for Turkey and its Surrounding Area (1938–2008). Boğaziçi University Publication, 2009; (1026).

[15] Kızılbuğa, S, Utkucu M, Yalçın H, Turan, F, Coşkun, Z., Kalkan, E, Pınar A. Monitoring and Relocating the Aftershock Sequence of the June 12, 2017 Karaburun-Lesvos Earthquake (Mw=6.3) VI. International Earthquake Symposium Kocaeli 2019 (IESKO 2019), Proceeding Book, p933-937 September 25-27, 2019, Kocaeli, TurkeyISBN:, 2019; 978-605-69403-1-6.

[16] Aktar, M., Karabulut, H., Özalaybey, S. and Childs, D. A conjugate strike-slip fault system within the extensional tectonics of Western Turkey. Geophysical Journal International, 2007; 171(3), 1363-1375.

[17] Jeffreys, H. and Bullen, K. E. Seismological tables//Brit. Assoc. for the advancement of Sci. London: Gray-Milne Trust, 1958; 65.

[18] Kikuchi, M. and Kanamori, H. Inversion of complex body waves—III. Bulletin of the Seismological Society of America, 1991; 81(6), 2335-2350.

[19] Özer, Ç., Polat, O., İzmir ve çevresinin 3-B kabuk hız yapısı. Gazi Üniversitesi Mühendislik-Mimarlık Fakültesi Dergisi, 2017, 32.3.

[20] Kikuchi, M., M. Nakamura, and K.Yoshikawa. Source rupture processes of the 1944 Tonankai earthquake and the 1945 Mikawa earthquake derived from low-gain seismograms, Earth Planets Space, 2003; 55, 159-172.

[21] Kohketsu, K. The extended reflectivity method for synthetic near-field seismogram. Journal of Physics of the Earth, 1985; 33(2), 121-131.

[22] Tiryakioğlu, İ., Aktuğ, B., Yiğit, C. Ö., Yavaşoğlu, H. H., Sözbilir, H., Özkaymak, Ç., et al. Slip distribution and source parameters of the 20 July 2017 Bodrum-Kos earthquake (Mw6. 6) from GPS observations. Geodinamica acta, 2018; 30(1), 1-14.

[23] Utkucu, M. and Kızılbuğa S. Analysis of the background seismicity and teleseismic source process of the July 20, 2017 Bodrum-Kos earthquake 5. International Conference on Earthquake Engineering and Seismology (5ICEES), 8-11 October 2019, METU Ankara, Turkey, 2019; 10 pp.